

Turbulent, steamy red supergiant winds

A. M. S. Richards¹, I. Bains², A. Bartkiewicz³, R. J. Cohen¹,
P. J. Diamond¹, S. Etoka¹, M. D. Gray⁴, E. E. Lekht⁵,
M. R. W. Mashedier⁶, E. Mendoza-Torres⁵, K. Murakawa⁷,
M. Szymczak³, H. J. van Langevelde^{8,9}, W. Vlemmings¹, and
J. A. Yates¹⁰

¹JBO, University of Manchester, SK11 9DL, UK. a.m.s.richards@manchester.ac.uk

²Centre for Astrophysics and Supercomputing, Swinburne University of Technology, PO Box 218, Hawthorn, Victoria 3122, Australia.

³Centre for Astronomy, Nicolaus Copernicus University, Torun, Poland.

⁴Dept. of Physics, University of Manchester, PO Box 88, Manchester M60 1QD, UK.

⁵INAOE, Apdo Postal 51 y 216, 72840 Tonantzintla, Puebla, Mexico.

⁶Department of Physics, Bristol University, Bristol, BS8 1TL, UK.

⁷Max-Planck-Institut für Radioastronomie, Auf dem Hugel 69, G-53121, Bonn, Germany.

⁸JIVE, Postbus 2, 7990 AA Dwingeloo, The Netherlands.

⁹Sterrewacht Leiden, Leiden University, Postbus 9513, 2300 RA Leiden, The Netherlands.

¹⁰UCL, Gower Street, London WC1E 6BT, UK.

Abstract. Rapidly-evolving red supergiants (RSG) lose half or more of their mass before ending their lives as supernovae. Masers allow us to study the mass loss from 4 nearby RSG in AU-scale detail using MERLIN and EVN/global VLBI. The water maser clouds are over-dense and over-magnetised with respect to the surrounding wind. In most cases, the brighter an individual maser component is the smaller its apparent (beamed) FWHM appears, as predicted for approximately spherical clouds. Individual water maser features have a typical half-life of 5-10 yr, but comparison with single dish monitoring suggests that the water vapour clouds themselves survive many decades (the water maser shell crossing time), within which the local masers wink on and off. OH mainline masers are found in the tenuous surrounding gas, overlapping the water maser shell, surrounded by OH 1612-MHz masers at a greater distance from the star.

Keywords. masers, stars: mass loss, late-type, supergiants, polarization, techniques: high angular resolution

1. Introduction

Stars more than about 8 times the mass of the Sun live fast and go out in a blaze of glory as a supernova. It is less well known that even before then, these stars contribute up to half of all the dust and a large proportion of light elements which enrich the interstellar medium and hence the next generation of star formation. This was especially important in the early universe owing to the rapid evolution of high-mass stars. Less than one in 200 stars are high-mass at birth, but they typically lose half their mass in the Red Super Giant (RSG) stage, over a few hundred thousand years. The stars lose mass through a combination of pulsation (with irregular periods of 2–5 yr) and radiation pressure on dust. They have no detectable rotation and the simplest “onion” model places spherical SiO, H₂O and OH maser shells at increasing distances from the star. We have studied four RSG, whose vital statistics are given in Table 1.

2. Water maser cloud measurements

We observed the H₂O emission at 22 GHz from all four sources using MERLIN, with a resolution of ≥ 10 mas. We measured maser emission in each channel by fitting 2D

Table 1. Red Supergiants studied. References not explicitly given are cited in the article listed for each star. The IRAS colour regions (C.R.) are defined in van der Veen & Habing (1988) and the $9.7\ \mu\text{m}$ silicate feature and dust morphologies are discussed in Monnier *et al.* (1999) and references therein. The OH 1612-MHz column gives the shell shape and approximate peak flux density.

RSG	D (kpc)	M_\star (M_\odot)	T_\star (K)	IRAS C.R.	Silicate feature	Dust morphology	OH 1612-MHz morphology	log(Jy)	References
S Per	2.2	20	2400	IIIa	emission	compact	biconical	0	RYC99
VX Sgr	1.7	10	2900	VII	emission	compact	\sim spherical	1	M+03
VY CMa	1.5	50	2700	VII	declining	complex	\heartsuit	2	RYC98
NML Cyg	2.0	50	3650	VIb	absorption	multiple shells	elongated, detached	2	RYC96, ED04

References: RYC96 Richards *et al.* (1996); RYC98 Richards *et al.* (1998); RYC99 Richards *et al.* (1999); M+03 Murakawa *et al.* (2003); ED04 Etoke & Diamond (2004).

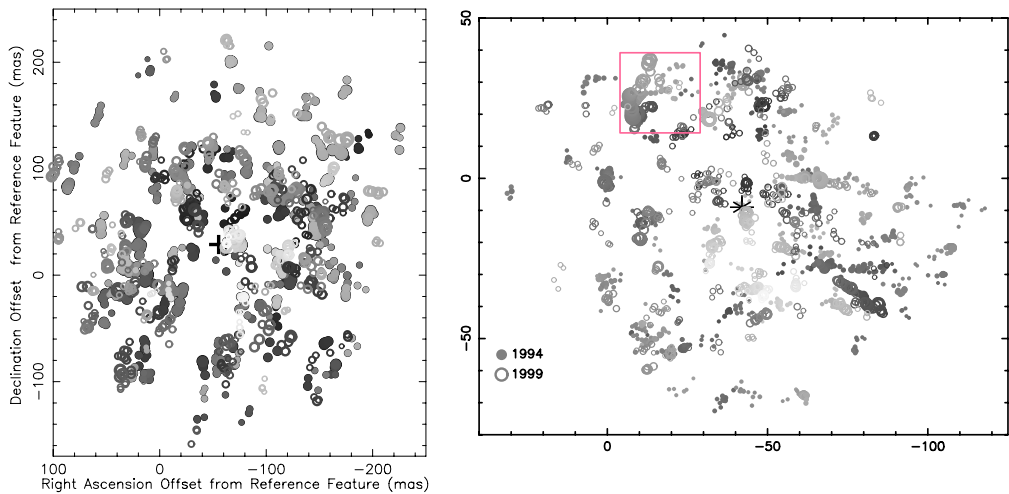


Figure 1. Positions of H_2O maser components around VX Sgr (*left*) and S Per (*right*) at 2 epochs. The darker (paler) symbols represent emission which is more red- (blue)-shifted with respect to V_\star and the size is proportional to $\log(\text{flux density})$.

Gaussian components, giving sub-mas position accuracy. We resolved the individual components in S Per and NML Cyg. Fig. 1 shows examples of H_2O maser shells.

2.1. Water maser shell sizes and densities

The water masers mostly occupy approximately spherical shells around each star, but with increasing signs of asymmetry, from a mild equatorial density enhancement in S Per to protruding jet-like features in NML Cyg. In each case 22-GHz emission traces strong acceleration away from the star; typically the outflow velocity doubles from 10 to 20 km s^{-1} over 100–200 or more AU, illustrated in Fig. 2. The inner rim of the shell is defined by the number density at which the masers are collisionally quenched, $n_q \approx 5 \times 10^{15} \text{ m}^{-3}$. The inner and outer radii and expansion velocities (r_i , r_o , v_i , v_o) were used to estimate the mass-loss rate $\dot{M}(n_q)$ if the number density of the whole wind was n_q at r_i . These properties are tabulated in Table 2, from which it can be seen that $\dot{M}(n_q)$ is unfeasibly large compared with other estimates or, indeed, RSG mass loss lifetimes.

Table 2. The mass loss rate measured from thermal emission $\dot{M}(\text{CO/IR})$ is compared with $\dot{M}(n_q)$; the latter is unfeasibly large, and an explanation is given in Section 2.2. The remaining columns give the inner and outer maser shell limits, see Table 1 for references.

RSG	$\dot{M}(\text{CO/IR})$ ($M_{\oplus} \text{ yr}^{-1}$)	$\dot{M}(n_q)$ ($M_{\oplus} \text{ yr}^{-1}$)	H_2O		OH 1665-MHz		OH 1667-MHz	
			r_i	r_o	r_i	r_o	r_i	r_o
S Per	3–60	930	55	165	80	80	570/175 ²	570/245 ²
VX Sgr	5–80	1900	95	320	130	130	540/1950 ³	540/1950 ³
VY CMa	65–115	3150	115	540 ¹	225	225	4500	10000
NML Cyg	35–60	5150	100	480 ¹	2400	3000	3200	5000

Footnotes ¹Including biconical/bipolar features; ²Observed in 1993/1999 ³Multiple shells;

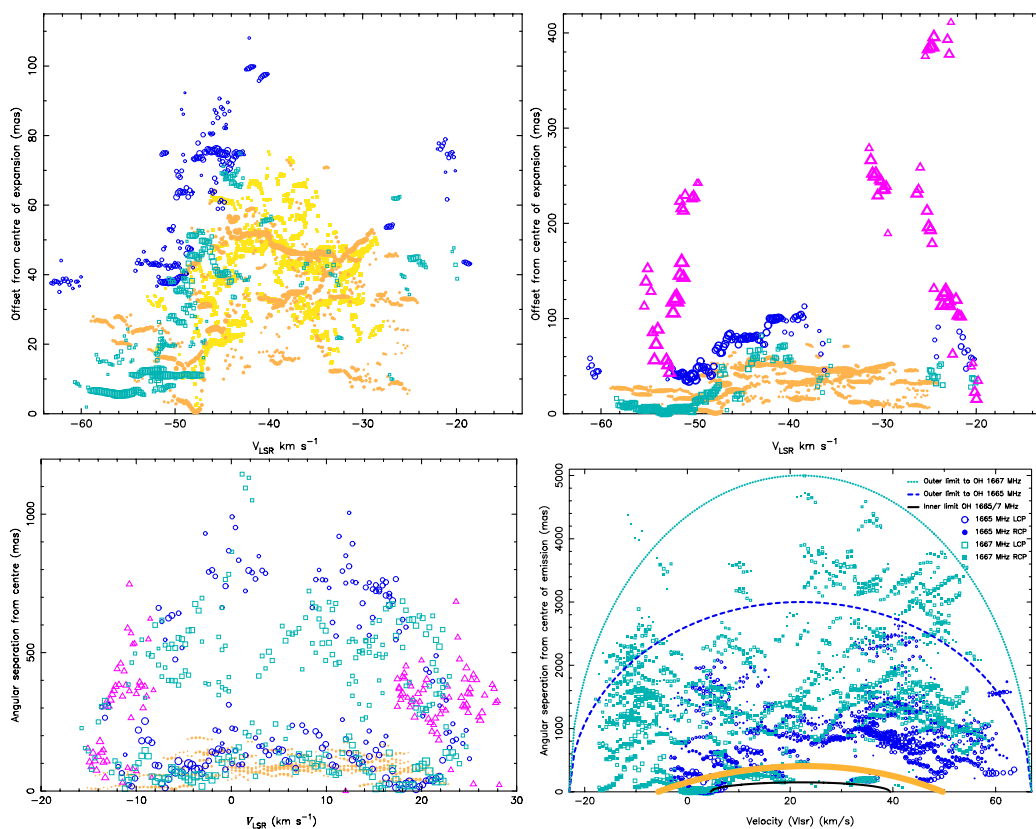


Figure 2. H_2O masers: pale filled circles; OH 1665/1667-MHz masers hollow squares; 1612-MHz masers: triangles. The V_{LSR} axes are centred on V_* . (top) S Per. (bottom)(left) VX Sgr, (right) VY CMa (only OH mainlines shown; the outer limit of H_2O emission is shown by the innermost arc).

2.2. Cloud sizes and survival

Fig. 1 shows that many maser components form ordered patterns with systematic velocity/position gradients, corresponding to an average cloud size of 20 AU. Some clouds have a total velocity extent 2 or more times the thermal line width and/or a total angular extent greater than the estimated gain length. This shows that the clouds are physically

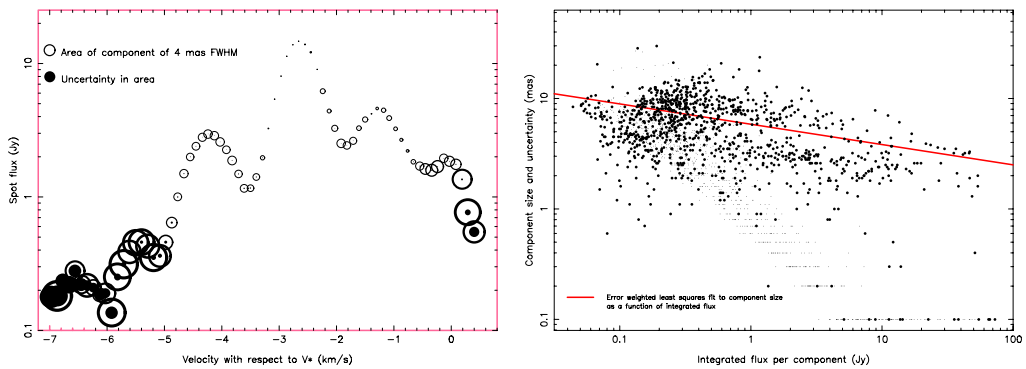


Figure 3. (*left*) Beamed areas of 22-GHz components in the feature of S Per boxed in Fig. 1. (*right*) FWHM of 22-GHz components (large symbols) and uncertainties (small symbols).

bounded, most likely by a density differential (Section 2.1). Each CSE contains about 50–100 H₂O maser clouds (assumed to be on average spherical), giving a volume filling factor of a few percent or less. The crossing time for the H₂O maser shell is ≈ 50 –80 yr, suggesting that a few clouds appear at r_i per stellar period and inject about 10–20 $M_{\oplus} \text{ yr}^{-1}$ into the CSE. This solves the mass-loss-rate problem, since the total mass in H₂O maser clouds is comparable to the mass-loss rate measured from thermal species. The surrounding gas number density needs to be $\sim 1/50$ or less of that in the clouds.

Comparison with other epochs of interferometry show that about half the maser clouds survive 5 or more years. Proper motions were measured for VX Sgr, VY CMa and NML Cyg. The velocities and accelerations are consistent with the observed V_{LSR} gradients. It is, however, surprising that the other half of the clouds vanish as the overall shell sizes imply that they survive for many decades. An explanation is provided by single-dish monitoring every few months by Lekht *et al.* (2005) using the Puschino telescope. We identified a bright feature in S Per seen at a very similar velocity and position in the 1994 and 1999 maps (the box in Fig. 1). The spectra show that this feature vanished just a few months after the 1994 MERLIN observations but re-appeared in 1998. This shows that the clouds themselves may survive any length of time, but detectable masers wink on and off, either due to local excitation conditions or to the beaming direction.

2.3. Direct measurements of maser beaming

The brightest maser emission is most strongly amplified and this leads to the narrowing of the apparent angular size of a single maser component propagating through an approximately spherical cloud (Elitzur 1992). The FWHM of the H₂O maser components in S Per is inversely proportional to their flux density illustrated in Fig. 3. A similar effect is seen for the OH mainline masers from VX Sgr and for three out of four AGB stars (Bains *et al.* 2003) but U Ori shows a direct relationship for the brightest masers at some epochs only. This could be explained if the masers originate from a shock front and there are other indications that this may be the case for U Ori.

3. OH maser distribution

The 1.6-GHz OH masers around all four RSG have been mapped by MERLIN at ≥ 120 mas resolution. The 1665 and 1667 MHz mainline masers from S Per and VX Sgr were also imaged using the EVN/global VLBI at ≥ 7 mas resolution. Fig 2 shows that the OH mainline masers overlap the H₂O maser shells in position and velocity in all CSEs apart

from NML Cyg. OH mainline emission close to V_* is seen between H_2O masers, showing that the apparent overlap is not just a projection effect of the front and back caps. No excited OH masers are detected, so the OH gas must be at a temperature ≤ 500 K and a number density $n \leq 10^{14} \text{ m}^{-3}$, consistent with the deduction in Section 2.2 that the surrounding gas is 1/50–1/100 less dense than the H_2O clouds.

We used Zeeman splitting of the OH mainline masers to measure a magnetic field strength of $\sim 0.3\text{--}3 \mu\text{T}$. The field strength in the H_2O maser clumps of these stars is $\sim 10\text{--}400 \mu\text{T}$ (Vlemmings *et al.* 2002, 2005). In S Per for example, the H_2O magnetic field is $\sim 10\text{--}20\times$ stronger than the OH magnetic field at 140 AU from the star. This suggests that the H_2O maser clumps have compressed, frozen-in fields where the magnetic field strength varies as $n^{\sim 0.3\text{--}0.5}$ (Mouschovias & Ciolek 1999).

4. Conclusions and future work

We have measured the apparent beamed size of individual 22-GHz H_2O maser components, finding that their FWHM is inversely proportional to the maser intensity. The components form distinct streaks which represent discrete water vapour clouds, typically 20 AU across. These take many decades to cross the H_2O maser shell but the 22-GHz emission from any single cloud may wink on and off several times during this lifetime. The H_2O clouds are 50 times denser than the surrounding gas. This explains how OH mainline masers can emanate at a similar distance from the star, but in more diffuse regions surrounding the H_2O masers, and how they appear to be associated with a much weaker magnetic field than the H_2O masers at a similar distance.

If the size of the clouds is extrapolated back to the stellar surface, allowing for an r^2 expansion in the wind, they would be born with a radius of $\sim 0.1R_*$. This could result from the ejection of matter associated with a convection cell bringing chemically enriched material to the surface, or with a star spot. Betelgeuse is the only RSG which has been so far resolved in detail; models (Freytag *et al.* 2002) produce structures on compatible scales. In future we will be able to resolve many more AGB and RSGs using *e*-MERLIN, the EVLA, VLBI and ALMA and even track individual clumps as they are ejected from the stellar surface, pass through the SiO maser zone, form dust, produce water masers and pass through OH mainline masers before joining the OH 1612-MHz maser shell.

References

- Bains, I., Cohen, R. J., Louridas, A., Richards, A. M. S., Rosa-González, D., & Yates, J. A. 2003, *MNRAS*, 342, 8
- Etoka, S., & Diamond, P. 2004, *MNRAS*, 348, 34
- Elitzur, M. 1992, *Astronomical Masers*, Kluwer
- Freytag, B., Steffen, M., & Dorch, B. 2002, *AN*, 323, 213
- Lekht, E. E., Rudnitskij, G. M., Mendoza-Torres, J. E., & Tolmachev, A. M. 2005, *A&A*, 437, 127
- Mouschovias, T. C., & Ciolek, G. E. 1999, in: C. J. Lada & N. D. Kylafis (eds.), *The Origin of Stars and Planetary Systems*, NATO ASIC Proc., 540, 305
- Monnier, J. D., Geballe, T. R., & Danchi, W. C. 1999, *ApJ*, 521, 261
- Murakawa, K., Yates, J. A., Richards, A. M. S., & Cohen, R. J. 2003, *MNRAS*, 344, 1
- Richards, A. M. S., Yates, J. A., & Cohen, R. J. 1996, *MNRAS*, 282, 665
- Richards, A. M. S., Yates, J. A., & Cohen, R. J. 1998, *MNRAS*, 299, 319
- Richards, A. M. S., Yates, J. A., & Cohen, R. J. 1999, *MNRAS*, 306, 954
- van der Veen, W. E. C. J. & Habing, H. J. 1988, *A&A*, 184, 125
- Vlemmings, W. H. T., Diamond, P. J., & van Langevelde, H. J. 2002, *A&A*, 394, 589
- Vlemmings, W. H. T., van Langevelde, H. J., & Diamond, P. J. 2005, *A&A*, 434, 1029